

# Combining optical and neural components in physiological visual image quality metrics as functions of luminance and age

**Gareth D. Hastings**

College of Optometry, University of Houston, Houston, TX, USA



**Jason D. Marsack**

College of Optometry, University of Houston, Houston, TX, USA



**Larry N. Thibos**

School of Optometry, Indiana University, Bloomington, IN, USA



**Raymond A. Applegate**

College of Optometry, University of Houston, Houston, TX, USA



Visual image quality metrics combine comprehensive descriptions of ocular optics (from wavefront error) with a measure of the neural processing of the visual system (neural contrast sensitivity). To improve the ability of these metrics to track real-world changes in visual performance and to investigate the roles and interactions of those optical and neural components in foveal visual image quality as functions of age and target luminance, models of neural contrast sensitivity were constructed from the literature as functions of (1) retinal illuminance (Trolands, td), and (2) retinal illuminance and age. These models were then incorporated into calculation of the visual Strehl ratio (VSX).

Best-corrected VSX values were determined at physiological pupil sizes over target luminances of  $10^4$  to  $10^{-3}$  cd/m<sup>2</sup> for 146 eyes spanning six decades of age. Optical and neural components of the metrics interact and contribute to visual image quality in three ways. At target luminances resulting in >900 td at physiological pupil size, neural processing is constant, and only aberrations (that change as pupil size changes with luminance) affect the metric. At low mesopic luminances below where pupil size asymptotes to maximum, optics are constant (maximum pupil), and only the neural component changes with luminance. Between these two levels, both optical and neural components of the metrics are affected by changes in target luminance. The model that accounted for both retinal illuminance and age allowed VSX, termed  $VSX(td, a)$ , to best track visual acuity trends (measured at 160 and 200 cd/m<sup>2</sup>) as a function of age (20s through 70s) from the literature. Best-corrected  $VSX(td, a)$  decreased by 2.24 log units between maximum and minimum target luminances in the youngest eyes and by 2.58 log units in the oldest.

The decrease due to age was more gradual at high target luminances (0.70 log units) and more pronounced as target luminance decreased (1.04 log units).

## Introduction

Visual image quality metrics (Chen, Singer, Guirao, Porter, & Williams, 2005; Thibos, Hong, Bradley, & Applegate, 2004) distil the visual system into two fundamental components: (1) an optical component derived from measured ocular wavefront error (with or without ophthalmic correction) and specific to a given eye under given conditions, and (2) a neural processing component originally derived from a representative photopic foveal neural contrast sensitivity function of a young eye measured with laser interferometry (Campbell & Green, 1965). The latter measurement is also now possible with adaptive optics (S. Elliott, Choi, Doble, Hardy, Evans, & Werner, 2009; Sabesan, Barbot, & Yoon, 2017) and can be derived analytically from wavefront error and total contrast sensitivity (Campbell & Green, 1965; Liu, Wang, Wang, Mu, & Zhao, 2010; Michael, Guevara, de la Paz, Alvarez de Toledo, & Barraquer, 2011).

Serving as objective surrogates for subjective measures of visual performance, visual image quality metrics have been employed in the study of accommodation (López-Gil, Martín, Liu, Bradley, Díaz-Muñoz, & Thibos, 2013), myopia (Collins, Buehren, & Iskander, 2006), postnatal visual development (Candy, Wang, & Ravikumar, 2009), and

Citation: Hastings, G. D., Marsack, J. D., Thibos, L. N., & Applegate, R. A. (2020). Combining optical and neural components in physiological visual image quality metrics as functions of luminance and age. *Journal of Vision*, 20(7):20, 1–20, <https://doi.org/10.1167/jov.20.7.20>.



refractive surgery outcomes (Bühren, Yoon, MacRae, & Huxlin, 2010), as well as in applications of extended depth of focus (Yi, Iskander, & Collins, 2010), eye models (Liu & Thibos, 2019), the design of intraocular lenses (Bonaque-González, Ríos, Amigó, & López-Gil, 2015), and predicting changes in visual performance (A. Ravikumar, Sarver, & Applegate, 2012; Shi, Applegate, Wei, Ravikumar, & Bedell, 2013a). Being more robust than measures such as residual diopters or root mean square (RMS) wavefront error in tracking visual performance (Cheng, Bradley, Ravikumar, & Thibos, 2010; Marsack, Thibos, & Applegate, 2004), visual image quality metrics have proven useful for optimizing objective refractions (Hastings, Marsack, Nguyen, Cheng, & Applegate, 2017; Martin, Vasudevan, Himebaugh, Bradley, & Thibos, 2011; A. Ravikumar, Benoit, Marsack, & Anderson, 2019) and have served as a benchmark for comparing both individualized and conventional ophthalmic corrections across modalities (unaided, spectacles, contact lenses) (Hastings, Applegate, Nguyen, Kauffman, Hemmati, & Marsack, 2019). Although the visual tasks, pupil sizes, and ages have differed across these applications, a constant neural component has typically been used in the visual image quality metrics. In this report, we examine the influence of these variable factors as a step toward increasing the efficacy of visual image quality metrics in the numerous applications mentioned above.

Additionally, the convention of reporting wavefront error at a common pupil size (American National Standards Institute, 2004) across individuals has meant that normative values of best-corrected visual image quality as a function of age were defined at fixed pupil sizes (Hastings, Marsack, Thibos, & Applegate, 2018). Although these have often been clinically satisfactory at the level of an individual patient, we also desire metrics that respect real-world physiological conditions. For example, the literature consistently reports decreasing visual performance with increasing age, typically measured through physiological pupils at constant luminances; examples include visual acuity (D. B. Elliott, Yang, & Whitaker, 1995; Owsley et al., 1983) and photopic and mesopic contrast sensitivity (D. B. Elliott, 1987; Owsley et al., 1983; Sloane et al., 1988a; Sloane et al., 1988b).

To improve the applicability of visual image quality metrics to individual eyes in real-world conditions, as well as to study best-corrected physiological visual image quality as a function of age, both components of the metrics (optical and neural) should account for the decrease in physiological pupil size with age (senile miosis). If those components are appropriately combined, one should be able to predict visual performance as a function of age, which, to our knowledge, has not been demonstrated. Treatment of the optical component is trivial, as methods exist to scale monochromatic wavefront error from a

maximum dilated pupil size (Schwiegerling, 2002) to a predicted physiological pupil size (Watson & Yellott, 2012). In contrast, the neural component is more challenging, primarily because decreasing physiological pupil size with age results in decreasing effective retinal illuminance (Trolands, td), and the literature agrees that neural processing (specifically, neural contrast sensitivity) varies with retinal illuminance (Coletta & Sharma, 1995; Kawara & Ohzu, 1977; Xu, Wang, Thibos, & Bradley, 2017). Also, there is the consideration of whether neural processing (at a constant retinal illuminance) decreases with age due to neuron loss or worsening signal-to-noise ratio; the relevant literature (which is divided on this second topic) is summarized in the Discussion section, and, in the absence of a definitive understanding of the impact of age, we study both cases here. As such, the effect of the neural component on visual image quality is specific to each multivariate combination of spatial frequency, retinal illuminance, and age.

To investigate the interactions of the optical and neural components of visual image quality metrics as a function of age and target luminance, we combined (1) predictions of physiological pupil size, (2) scaling of wavefront error aberrations, and (3) models of neural contrast sensitivity derived from literature. We compared two models of neural contrast sensitivity: one a function of spatial frequency and retinal illuminance, and the other a function of spatial frequency, retinal illuminance, and age (decade age-groups). In doing so, visual image quality metrics provide a unique perspective from which to examine the roles and interactions of optical and neural factors as target luminance and age change. We show that these components interact and contribute to visual image quality differently over three luminance domains and that, by combining appropriate optical and neural components, visual image quality metrics can mimic the relative change in visual acuity with age reported in literature.

## Methods

### Wavefront error, target luminance, physiological pupils, and retinal illuminance

Wavefront aberration data were collected during the Texas Investigation of Normal and Cataract Optics study (Applegate, Donnelly, Marsack, Koenig, & Pesudovs, 2007), which followed the tenets of the Declaration of Helsinki and obtained signed informed consent approved by the University of Houston Institutional Review Board. Briefly, Applegate et al. (2007) studied the change in wavefront aberration structure as crystalline lens opalescence

increased naturally with age. Individuals with cortical and/or posterior subcapsular cataracts graded as  $>2$  on the Lens Opacities Classification System III (LOCS-III) (Chylack et al., 1993) were excluded, as were applicants with any previous ocular surgery, pathology, or abnormality (such as strabismus or amblyopia).

Wavefront errors were measured over maximum dilated pupils (one drop 1% tropicamide and one drop 5% neosynephrine) of the preferred eyes of 146 normal healthy individuals between 20 and 80 years of age using a custom Shack–Hartmann wavefront sensor. Resulting wavefront errors were fit with a 10th radial order normalized Zernike polynomial expansion. These measured wavefront errors were scaled (Schwiegerling, 2002) to physiological pupil sizes predicted (Watson & Yellott, 2012) over a range of photopic and mesopic target luminances ( $10^{-3}$  to  $10^4$  in increments of 1 log  $\text{cd}/\text{m}^2$ ,  $10^{-3} \text{ cd}/\text{m}^2$  being the lower bound of cone sensitivity) (Roufs, 1978). The term *mesopic* is used despite that neural contrast sensitivity and visual image quality in this paper are confined to the (rod-free) fovea because foveal cones are still functional at those luminance levels (Roufs, 1978). Inputs to the physiological pupil size calculations were for *binocular* (rather than *monocular*) viewing and a  $60^\circ$  adapting field size (Watson & Yellott, 2012). Additionally, target luminance of  $160 \text{ cd}/\text{m}^2$  was evaluated for comparison with specific literature. A small proportion of eyes did not dilate to the physiological pupil sizes predicted for low target luminances (Appendix A); in these cases, the maximum dilated pupil size was used instead to avoid scaling aberrations to larger pupil sizes than were measured. Accommodation could decrease pupil size beyond that which is predicted by luminance and age; throughout this paper, we assume accommodation to be relaxed. Retinal illuminance for each eye at each target luminance was calculated as the product of target luminance and predicted physiological pupil area.

### Models of neural contrast sensitivity as a function of spatial frequency, retinal illuminance, and age

Neural contrast sensitivity data for six retinal illuminances between 0.9 and 9000 td were extracted from Figure 1 of Xu et al. (2017) (replotted in our Figure 1A) and fit with a two-dimensional regression using *polyfitn* (D'Errico, 2016) in MATLAB (MathWorks, Natick, MA), with  $R^2 = 0.9958$ , degrees of freedom remaining = 319, RMS error of fit = 0.046 log neural contrast sensitivity. Xu et al. (2017) derived neural contrast sensitivity from total contrast sensitivity data reported by Rovamo, Mustonen, and Näsänen (1994)

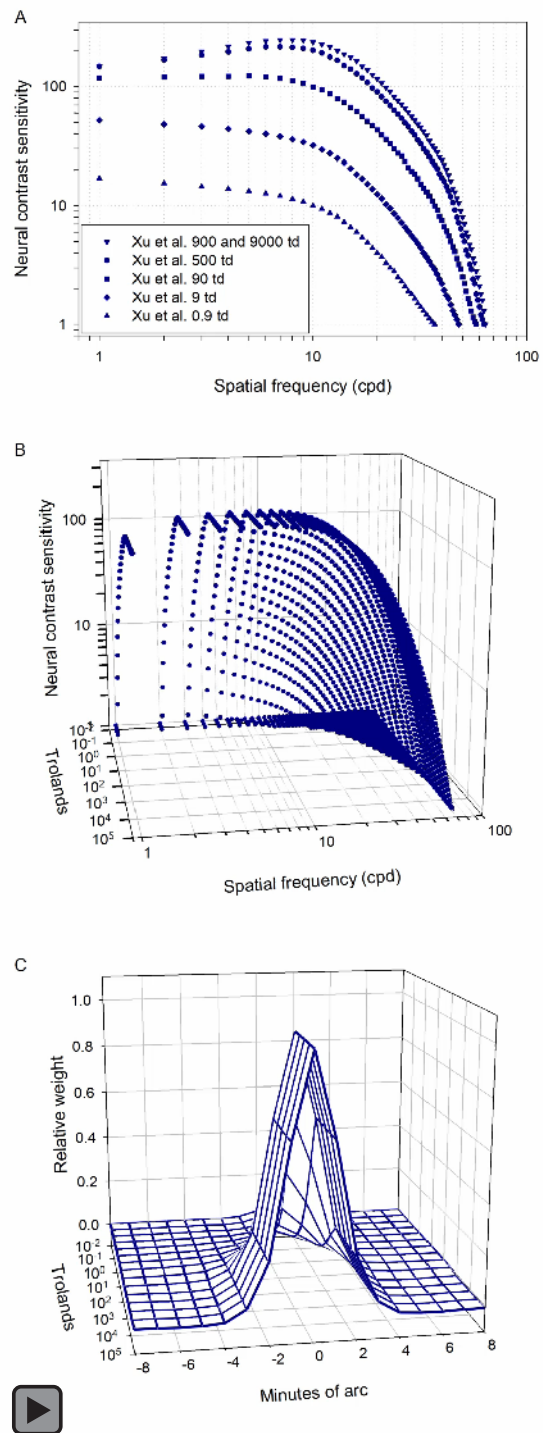


Figure 1. Neural contrast sensitivity as a function of retinal illuminance. (A) Neural contrast sensitivity functions at six retinal illuminance levels from Xu et al. (2017) that were fit with a two-dimensional regression to form (B), a model of neural contrast sensitivity as a function of spatial frequency (cycles per degree) and retinal illuminance (Trolands). (C) Neural weighting functions used in the *VSX(td)* metric, obtained via inverse Fourier transform of the functions in (B).

that were computed using their theoretical model. Rovamo et al. (1994) validated their model by comparing its behavior with empirical data reported by Van Nes and Bouman (1967) and Banks, Geisler, & Bennett (1987). Xu et al. (2017) scaled the fitted polynomial for the 500-td function to agree with the function of a 27-year-old from Campbell and Green (1965) that was historically used in visual image quality metrics. The same relative neural contrast sensitivity scaling factors were applied to functions at other levels of retinal illuminance. When incorporating an age-related factor, these neural functions (from Xu et al., 2017) were taken as representing the 20- to 29-year-old age-group across different levels of retinal illuminance.

Neural contrast sensitivity data for decade age-groups at one retinal illuminance (160 td) were extracted from Figure 3 of Nameda, Kawara, and Ohzu (1989) and are shown in our Figure 2A. At each spatial frequency, the sensitivities of the 30 to 39, 40 to 49, 50 to 59, and 60 to 69 age-groups were each divided by that of the 20 to 29 age-group to generate decade age-group multipliers relative to the 20 to 29 years group (Figure 2B). At each spatial frequency the multipliers were linearly extrapolated in MATLAB to determine an age multiplier for the >70 year old age group. Linear extrapolation was used because change in neural contrast sensitivity with age was approximately linear within each spatial frequency (Morrison & McGrath, 1985; Nameda et al., 1989) and is in agreement with anatomical (Balazsi, Rootman, Drance, Schulzer, & Douglas, 1984; Curcio, Millican, Allen, & Kalina, 1993; Devaney & Johnson, 1980; Gao & Hollyfield, 1992) and performance (D. B. Elliott et al., 1995; Owsley et al., 1983; Porciatti, Burr, Morrone, & Fiorentini, 1992) measures that change approximately linearly with age. We also evaluated an alternate double-exponent model (Movshon & Kiorpes, 1988; Wensveen, Smith, Hung, & Harwerth, 2011; Wilson, 1978) and found it fit the neural contrast sensitivity data nearly as well as the polynomial model at any single retinal illuminance. Given that the polynomial method simultaneously included retinal illuminance as a fitting parameter, it was preferred for this work.

### Visual image quality metric: the visual Strehl ratio

The contents of this paper are applicable to any visual image quality metric that incorporates a neural contrast sensitivity weighting function; conversely, metrics that do not incorporate neural weighting are referred to as optical or retinal image quality metrics. To illustrate the developments made here, the visual Strehl ratio (VSX) (Thibos et al., 2004) is used. Historically,

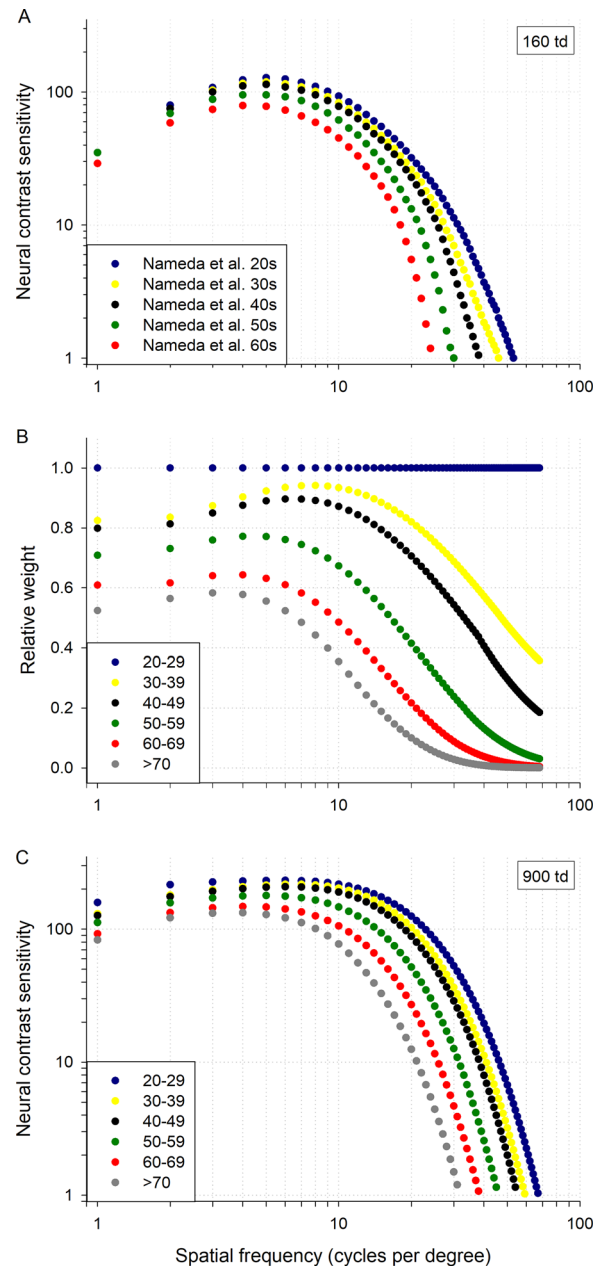


Figure 2. Relative neural contrast sensitivity as a function of age. (A) Neural contrast sensitivity functions at 160 td from Nameda et al. (1989) for decade age-groups were divided (at each spatial frequency) by the sensitivity of the “20s” age-group to derive (B), decade age-group multipliers as a function of spatial frequency, which weight the model defined in Equation 5 and Figure 1 and determine the neural contrast sensitivity functions that (after Fourier transformation) are used in the  $VSX(td,a)$  metric. The age-group multipliers in (B) are numerically defined in Appendix B. Panel (C) shows an example of the function for 900 td being weighted for all age-groups; the function labeled as 20–29 is the function at 900 td in Figure 1B.

VSX has been calculated as the ratio of the volume of the point spread function (PSF) of an eye (determined from a wavefront error measurement at a specific pupil size) to the volume of the diffraction-limited PSF for the same pupil size, where both PSFs are first weighted by the inverse Fourier transform of a neural contrast sensitivity function from Campbell and Green (1965). More recently, using a constant denominator, such as a diffraction-limited 3-mm pupil, across all eyes has been advocated (López-Gil et al., 2013; Sreenivasan, Aslakson, Kornaus, & Thibos, 2013) and we employed such normalization here. The advantage is principally twofold. First, for most sphero-cylindrically corrected typical eyes, a 3-mm pupil provides a good balance between optical aberrations and diffraction. Second, metrics using a 3-mm denominator better captures loss in visual image quality due to diffraction at pupil diameters smaller than 3 mm.

Although VSX (like other visual image quality metrics) incorporated a single neural contrast sensitivity measurement drawn by eye through method-of-adjustment data from one 27-year-old individual in 1965 (Campbell & Green, 1965), it has been shown to be predictive of subjective best focus (Cheng, Bradley, & Thibos, 2004; Marsack et al., 2004; Martin et al., 2011; Thibos et al., 2004), able to predict sphere, cylinder, and axis spectacle prescriptions that performed equivalently to subjective refraction (Hastings, Marsack, Nguyen, Cheng, & Applegate, 2017; A. Ravikumar et al., 2019), and has been used to evaluate conventional and wavefront-guided contact lenses (Hastings et al., 2019; Hastings et al., 2020; Shi, Queener, Marsack, Ravikumar, Bedell, & Applegate, 2013b). Changes in the logarithm of the VSX have been well correlated with changes in visual performance (Schoneveld, Pesudovs, & Coster, 2009) and especially with logMAR visual acuity (A. Ravikumar, Applegate, Shi, & Bedell, 2011; A. Ravikumar et al., 2012) independent of underlying pupil size and wavefront error.

To respect how the neural contrast sensitivity weighting function of the metric changes with retinal illuminance, as well as with both retinal illuminance and age, we defined two modifications of VSX that are presented in parallel throughout the paper. The metric referred to as  $V SX(td)$  is calculated as

$$V SX(td) = \frac{\iint PSF_{(Eye)}(x, y) \cdot N_{(Trolands)}(x, y, t) dx dy}{\iint PSF_{DL(3mm)}(x, y) \cdot N_{(900td)}(x, y) dx dy} \quad (1)$$

where  $PSF_{(Eye)}$  is at the physiological pupil size to which the wavefront error was scaled, the neural weighting function ( $N$ ) in the numerator is specific to the retinal illuminance (product of physiological pupil size and target luminance) of the condition,  $PSF_{DL(3mm)}$  is for a diffraction-limited 3-mm pupil diameter, and the neural

weighting function in the denominator is from the (maximum) neural contrast sensitivity function defined at 900 td.

The metric referred to as  $V SX(td, a)$  is defined as

$$V SX(td, a) = \frac{\iint PSF_{(Eye)}(x, y) \cdot N_{(Trolands, Age)}(x, y, t, a) dx dy}{\iint PSF_{DL(3mm)}(x, y) \cdot N_{(900td, 20-29y/o)}(x, y) dx dy} \quad (2)$$

where  $PSF_{(Eye)}$  and both parts of the denominator are the same as  $V SX(td)$  above, and the neural weighting function in the numerator is specific to both retinal illuminance and the age of the eye.

Wavefront error measurements were used to compute the PSF of each eye at each physiological pupil size using standard Fourier optics calculations (Goodman, 1996) but were not used to compute the neural transfer function ( $N$ ) using the analytical method mentioned in the Introduction because that would have confounded the calculation of visual image quality for the following reason: The analytic method (Campbell & Green, 1965) computes the neural contrast sensitivity function as

$$\begin{aligned} & \text{Neural contrast sensitivity function} \\ & = \text{Total contrast sensitivity function} / \\ & \quad \text{Optical transfer function} \end{aligned} \quad (3)$$

The optical transfer function (OTF) is the Fourier transform of the PSF, and a spatial neural weighting function could be determined by inverse Fourier transformation (IFT) of the computed neural contrast sensitivity function in Equation (3), which could be rewritten in the spatial domain as

$$N = IFT(\text{Total contrast sensitivity function}) / PSF \quad (4)$$

Calculating a neural weighting function in this manner is not problematic in itself; however, if this function, which is calculated from a particular wavefront error, is used to weight a PSF calculated from the same wavefront error, such as would be done in calculation of a visual image quality metric (Equation 1 or 2), then the effects of optical aberrations (PSF) are cancelled and lost. For example, aberrations worsen the PSF, which increases the computed  $N$ , but that increase is nullified when  $N$  is multiplied by the PSF to compute visual image quality. Clearly, the same shortcoming exists if calculations are performed in the Fourier or frequency domain using analogous metrics such as visual Strehl ratio based on the optical transfer function (VSOTF). To avoid this problem, we used independent sources for measured neural contrast sensitivity functions as described above.

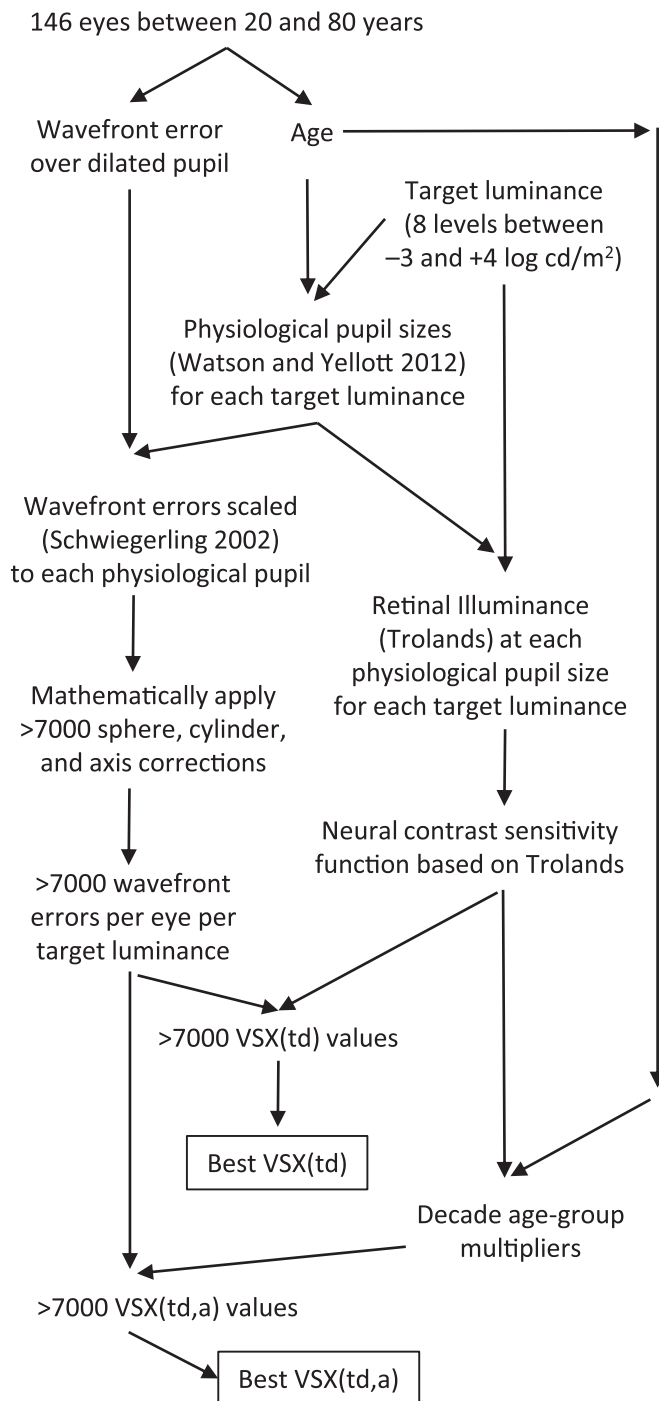


Figure 3. Flow diagram of methods beginning with measured wavefront error and culminating in best-corrected visual image quality metric values for  $VSX(td)$  and  $VSX(td,a)$ .

## Metric calculations

Simulated through-focus experiments using  $VSX(td)$  and  $VSX(td,a)$  were performed. For each scaled wavefront error (including higher- and lower-order aberrations) of each of the 146 eyes at the physiological pupil sizes predicted for each target luminance, a spherical dioptic value was calculated from

second-order Zernike defocus. Around this value, a range of sphere, cylinder, and axis prescriptions was mathematically applied that spanned sphere values from  $-1.50D$  to  $+1.50D$  in  $0.25D$  steps (centered on the second-order Zernike defocus) and cylinder values from  $0D$  up to  $-1.50D$  beyond the second-order Zernike cylinder in  $0.25D$  steps and  $2^\circ$  axis increments. This resulted in at least 7000 prescriptions being objectively applied to the wavefront error of each eye at each predicted physiological pupil size condition. Best-corrected  $VSX(td)$  and  $VSX(td,a)$  metric values were taken as the maximum metric value obtainable with any of these sphere, cylinder, and axis combinations. Similarly, the sphere, cylinder, and axis corrections that maximized the optical Strehl ratio (no neural weighting) and minimized total residual RMS wavefront error were also determined from the same simulated through-focus experiment.

## Results

Results are organized according to the two phases in which the modeling was accomplished. The prediction of physiological pupil size (Watson & Yellott, 2012) and the definition of the models of neural contrast sensitivity are presented first because they were required prior to the modeling of the visual image quality metric components, which is presented second.

### Retinal illuminance and physiological pupil size

Decreasing (or increasing) luminance always results in decreased (increased) retinal illuminance at all ages despite the compensatory enlargement (constriction) of pupil size. Calculated physiological pupil diameters ranged from 2.47 mm for the oldest eye (78.4 years) at the brightest target luminance ( $10^4$  cd/m<sup>2</sup>) to 8.05 mm for the youngest eye (21.8 years) at the dimmest target luminance ( $10^{-3}$  cd/m<sup>2</sup>).

### Models of neural contrast sensitivity as a function of spatial frequency, retinal illuminance, and age

The derived model of neural contrast sensitivity (see Methods) used in the  $VSX(td)$  metric is a polynomial function of two variables:

$$\begin{aligned} \log nCS(t, f) &= -0.009t^4 - 0.020t^3f + 0.062t^3 + 0.013t^2f^2 \\ &+ 0.107t^2f - 0.203t^2 - 0.115tf^3 + 0.209tf^2 \\ &- 0.142tf + 0.62t - 0.934f^4 + 2.490f^3 \\ &- 2.668f^2 + 0.869f^1 + 1.221f \end{aligned} \quad (5)$$

where  $\log nCS$  is the base-10 logarithm of neural contrast sensitivity,  $t$  is retinal illuminance (log Trolands), and  $f$  is spatial frequency (log cycles per degree). The MATLAB script (to greater decimal precision) for the above equation is included in [Appendix B](#). This model and the associated inverse Fourier transforms (PSF weighting functions) are shown in [Figures 1B](#) and [1C](#) for the range of Troland values that resulted from target luminance values of  $10^{-3}$  to  $10^4$   $\text{cd/m}^2$  at physiological pupil sizes for the population of eyes studied here.

The weighting functions used in the  $VSX(td,a)$  metric each started with calculation of a neural contrast sensitivity function at a specific retinal illuminance using [Equation 5](#) (the same function used in the  $VSX(td)$  metric). Thereafter, that function was weighted at each spatial frequency by the relevant decade age-group multiplier (based on the age of the eye), as shown in [Figure 2](#). Numeric definitions of the age multipliers are included in [Appendix B](#). The resulting (weighted) neural contrast sensitivity function (specific to retinal illuminance and age) underwent an inverse Fourier transform and was incorporated into the numerator of [Equation 2](#).

Peak neural contrast sensitivity decreased with increasing age and occurred at a lower spatial frequency. Sensitivity at high spatial frequencies particularly reduced with age. These behaviors are in agreement with well-established literature and merely indicate that the fitting of the neural functions maintained these characteristics.

## Relative contributions of optical and neural metric components as a function of target luminance

Physiological visual image quality is determined by the interaction and relative contributions of the optical and neural components of the metric in three ways defined by target luminance. These are identical for  $VSX(td)$  and  $VSX(td,a)$ . In [Figure 4](#), lines designating the transition of these three zones are superimposed on the data described in the next section.

### Above 900 td retinal illuminance

At high photopic target luminances that result in  $\geq 900$  td retinal illuminance at physiological pupil sizes, the neural component is constant ([Van Nes & Bouman, 1967](#); [Xu et al., 2017](#)). As luminance changes above this level, visual image quality is influenced solely by changes in the optical component—that is, optical aberrations that increase (or decrease) with the increase (decrease) in pupil size in response to decreasing (increasing) luminance. This luminance threshold varied with age.

The target luminance at which 900 td was reached and above which neural processing became constant changed from  $10^{1.58}$   $\text{cd/m}^2$  in the youngest eyes to  $10^{1.98}$   $\text{cd/m}^2$  in the oldest eyes. This is indicated by the red lines in [Figure 4](#).

### Below maximum physiological pupil size

At the opposite end of the target luminance range, at levels below those where maximum physiological pupils occur, the optical component is constant as luminance decreases further (because pupil size is already at a maximum) and visual image quality is influenced only by changes in the neural processing component, which decreases with the decrease in luminance ([Figure 5C](#)). Scotopic physiological pupil unrest (hippus) in alert individuals is on the order of 0.25 mm ([Yoss, Moyer, & Hollenhorst, 1970](#)); therefore, in this modeling, maximum pupil diameter was taken as being within 0.25 mm of the physiological pupil diameter defined by the [Watson and Yellott \(2012\)](#) model at  $10^{-4}$   $\text{cd/m}^2$ . This point also varied with age, occurring at approximately  $10^{-1.38}$  and  $10^{-0.56}$   $\text{cd/m}^2$  for the youngest and oldest eyes, respectively, and is indicated by the blue lines in [Figure 4](#).

### Between 900 td and maximum pupil size

Between high photopic luminances producing 900 td and low mesopic luminances that result in maximum physiological pupil sizes, both optical and neural components change when target luminance changes and both influence visual image quality. This is the region between the blue and red lines in [Figure 4](#). As target luminance decreases within this range, physiological pupil size increases, which increases aberrations, and retinal illuminance decreases, which reduces the neural contrast sensitivity function (as shown in [Figure 1](#)).

## Best-corrected physiological visual image quality

In agreement with the prevailing qualitative clinical understanding of visual quality, best  $VSX(td)$  and  $VSX(td,a)$  occurred in young eyes (20 to 29 age-group) at high photopic luminances ( $10^4$   $\text{cd/m}^2$ ) that produced small physiological pupils. When the neural weighting function accounted only for retinal illuminance,  $VSX(td)$ , visual image quality was relatively constant across age for all target luminances ([Figure 4A](#)). The addition of age-specific weighting to the neural component— $VSX(td,a)$ —resulted in a decrease in visual image quality with age (from 20s to 70s) that was more gradual at high target luminances (0.70 log units) and more pronounced as luminance decreased (1.04 log units) ([Figure 4B](#)). Retinal illuminance had a larger

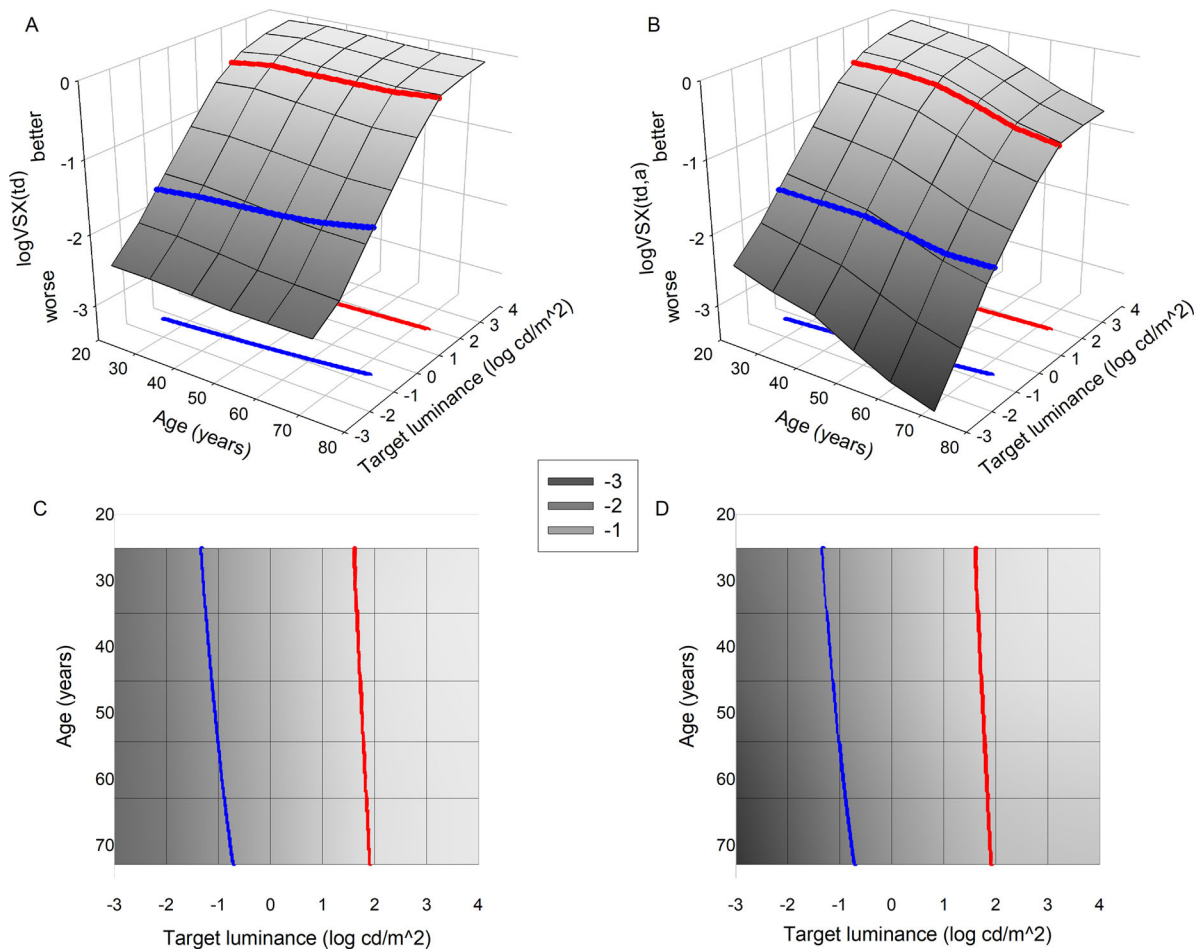


Figure 4. Mean best-corrected visual image quality for each decade age-group and target luminance where  $VSX(td)$  and  $VSX(td,a)$  metrics were calculated at the physiological pupil size (Watson & Yellott, 2012) of each subject for each luminance, and the neural weighting function (from Figures 1 and 2) was specific to retinal illuminance (A and C) and retinal illuminance and age (B and D). Colored lines designate three luminance ranges where optical and neural factors interact differently. (1) Above the red lines, target luminances and physiological pupil sizes result in retinal illuminances (not explicitly shown) of at least 900 td; here, neural contrast sensitivity is constant as target luminance changes and only optical aberrations affect visual image quality. (2) Below the blue lines are low mesopic luminances where maximum physiological pupils occur; here, optics are constant (maximum pupil), as luminance changes and only neural processing affects visual image quality. (3) At target luminances between those two lines, optical and neural factors both change as luminance changes. (C) and (D) show top views of (A) and (B) and illustrate the effects of senile miosis; that is, 900 td and maximum physiological pupil sizes are reached at higher luminance as age increases, meaning that as luminance changes, the role of the optical component decreases with age relative to that of the neural component, which becomes more relevant with increasing age.

effect than age on best-corrected  $VSX(td,a)$ , resulting in a 2.24-log unit decrease between maximum ( $10^4 cd/m^2$ ) and minimum ( $10^{-3} cd/m^2$ ) target luminances in the youngest eyes and a 2.58-log unit decrease in the oldest.

### Relative contributions of optical and neural metric components as a function of age

At any fixed pupil size, aberrations of the eyes increased with age and at a greater rate for larger pupils;

fixed pupils have been discussed in detail previously (Applegate et al., 2007). Senile miosis is a significant age-related phenomenon that had a protective influence on effective physiological aberrations (Figure 5A); that is, at high target luminance levels the magnitude of aberrations increased (worsened) only slightly with age and at lower luminances decreased (improved) slightly with age (due to maximum physiological pupil size decreasing with age). Although being of lower magnitude, the aberrations of older eyes interacted such that retinal image quality, as measured by the Strehl ratio, generally decreased (worsened) with increasing age (Figure 5B); increased diffraction at

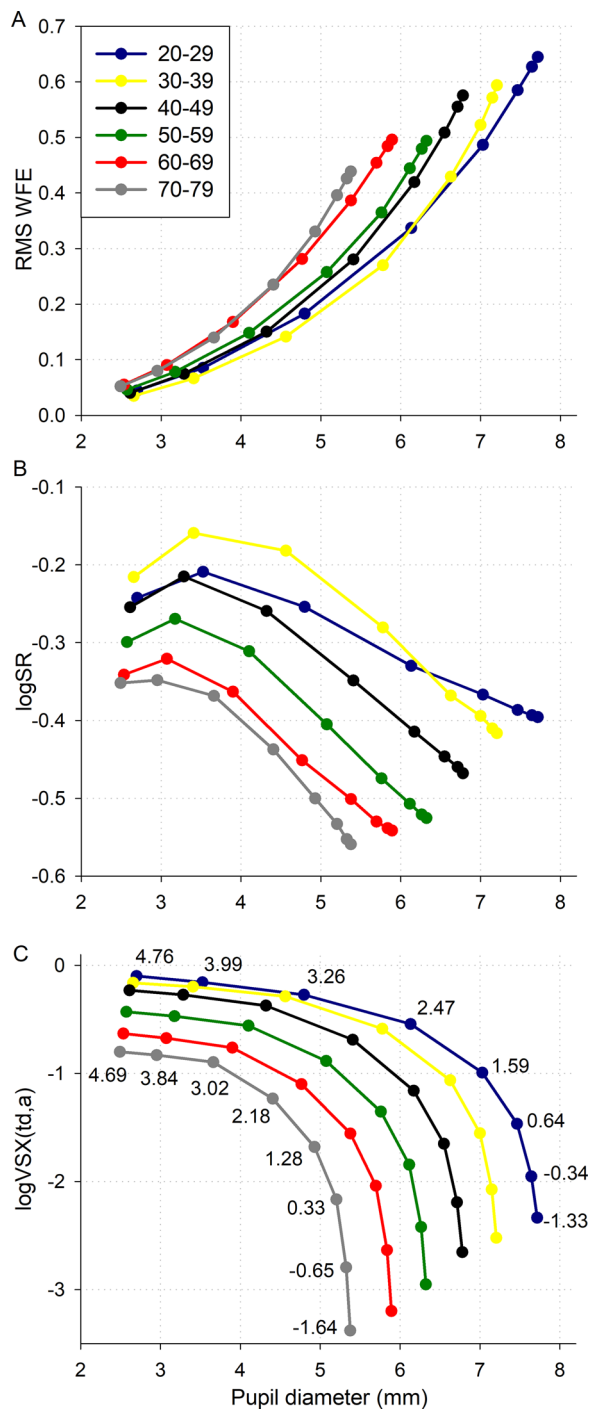


Figure 5. Combining optical and neural components of visual image quality at physiological pupil diameters. (A) Total RMS wavefront error (WFE) as a function of physiological pupil diameter after best sphero-cylindrical correction for each age-group at each target luminance (from  $10^{-3}$  to  $10^4$  in increments of 1 log cd/m<sup>2</sup>, corresponding to the eight points on each line in each panel but not explicitly shown). (B) Best-corrected base-10 logarithm of the Strehl ratio (logSR) (no neural weighting). The detrimental effect of diffraction is visible for small pupil sizes. (C) Best-corrected log  $VSX(td,a)$ . For any age-group, as pupil size increases (abscissa) in response to

smaller physiological pupils also contributed to this effect. The optical component (Figures 5A and 5B) improved slightly from the 20 to 29 age-group to the 30 to 39 age-group; although this might simply be an idiosyncrasy of the dataset, a similar trend has been independently reported (Brunette, Bueno, Parent, Hamam, & Simonet, 2003).

Figure 5C illustrates changes in visual image quality in terms of physiological pupil diameters (rather than target luminance as in Figure 4), which were more similar across different age-groups at high target luminance (less than 1-mm difference) and became more different (greater than 2 mm) with decreasing luminance. Despite physiological pupil sizes at maximum and minimum target luminances differing by less in older eyes than in younger eyes, the oldest eyes showed a greater change in  $VSX(td,a)$  visual image quality (2.58 log units) than the youngest eyes (2.24 log units) as a function of target luminance due to worsening of the neural component (due to both lower retinal illuminance and increased age). As mentioned above, these changes as a function of target luminance were greater than those as a function of age at a constant target luminance (0.70 log units at the highest luminance and 1.04 log units at the lowest).

Over the ranges modeled here, as target luminance decreased the role of the neural component in visual image quality became more relevant as age increased. The high luminance point at which 900 td retinal illuminance occurs and neural processing begins to vary with target luminance occurs sooner (at a higher target luminance) as age increases. The point where the optical component becomes constant (maximum physiological pupil size) and only luminance-driven changes in the neural component affect visual image quality also occurs sooner (at higher luminance) as age increases. Although senile miosis (at a given target luminance) mitigated much of the change in the optical component with age (the Strehl ratio generally differed by less than 0.3 log units between the youngest and oldest eyes), the

← decreasing target luminance, the log  $VSX(td,a)$  metric value decreases due to increasing aberrations and a worsening neural weighting function (lower retinal illuminance; log Trolands, product of target luminance and physiological pupil size for the 20 to 29 and >70 age-groups, are annotated next to their respective curves). When physiological pupil size asymptotes to a maximum, the optics remain essentially constant (maximum pupil) as luminance decreases further, and the neural weighting function is responsible for the further decrease in visual image quality (ordinate), which is approximately 2 log units greater than the decrease in the optical component alone for young eyes and 2.5 log units for older eyes (B). →

neural component worsened due to both lower retinal illuminance and increasing age, and  $VSX(td,a)$  differed by approximately 1 log unit between the youngest and oldest eyes, which is more representative of actual performance losses, as described in the following section.

## Discussion

We sought to quantitatively describe physiological visual image quality as a function of target luminance, as well as of target luminance and age. Because image quality cannot be directly measured on the retina (the eye is a closed imaging system), modeling was performed where physiological pupil sizes were calculated for a large dataset of eyes, wavefront error aberrations were scaled to those physiological pupil sizes, and two models of neural contrast sensitivity were developed from the literature and used to modify calculation of the visual image quality metric VSX.

Because the purpose of visual image quality modeling is to provide a quantitative surrogate for tedious psychophysical measurement of visual performance, we first defend the datasets used in the modeling by showing them to be generally representative of the broader literature. Then, quantitative descriptions of visual image quality metric values as a function of age are extracted from the Results and compared with independently measured visual acuity as a function of age. Finally, given the good ability of the metric and modeling to track visual acuity when optical and neural components are appropriately combined, applications and limitations of the modeling and the models are discussed.

### Comparison with literature: models of neural contrast sensitivity

The models should be taken as representing mean neural contrast sensitivity around which there will undoubtedly be variability in individual performance. A challenge of unifying neural contrast sensitivity literature—even if comparisons are limited to laser interferometry studies (and methods such as adaptive optics are not considered)—is that the sophistication of technology has evolved over time, and certain characteristics of the systems, such as coherence fractions (Williams, 1985), were often not considered or reported. Most studies of neural contrast sensitivity were performed at a single retinal illuminance level, and often this value, as well as the ages of subjects, were not reported.

The models presented here were constructed using data from Xu et al. (2017) (scaled to match Campbell and Green (1965)) and Nameda et al. (1989), and show good agreement (Figure 6A) with neural contrast sensitivity curves at various retinal illuminances from Kawara and Ohzu (1977), Coletta and Sharma (1995), and Still (1989). The model corresponds to approximately the best performance of 95 eyes reported by Dressler and Rassew (1981) at 1000 td and the worst performance of six eyes reported by Williams (1985) at 500 td; in Figure 6B, mean data from those studies are compared with the model. The neural contrast sensitivity functions measured by Williams (1985) were better than all of the literature with which they compared themselves, and Dressler and Rassew pooled data across six decades, which likely contributed to the lower levels they reported. The models in the present study, like the data upon which they are based (Xu et al., 2017), agree with other literature (Van Nes & Bouman, 1967) in that neural contrast that neural contrast sensitivity is constant at retinal illuminances above 900 td.

The wavelength of monochromatic light differed across the studies mentioned above and compared in Figure 6; however, this is theoretically irrelevant when working in the photometric unit of Trolands, as the conversion of radiometric power to Trolands incorporates weighting by a luminosity function ( $V^*\lambda$ ) (Bass, 1995; Wyszecki & Stiles, 2000). Although the luminosity function changes with age (Sagawa & Takahashi, 2001) due to shifts in the transmission of ocular media (Delori & Burns, 1996; Weale, 1988), we feel this is not significant here because the studies being compared did not measure neural contrast sensitivity using very short wavelength light (which is where the greatest change is found).

### Comparison with literature: best-corrected physiological visual image quality

Sphero-cylindrically best-corrected metric values as functions of age (for physiological pupils) at 160 cd/m<sup>2</sup> were compared with (sphero-cylindrically) best-corrected visual acuity recorded with physiological pupils and target luminances of 160 (D. B. Elliott et al., 1995) to 200 (Owsley et al., 1983) cd/m<sup>2</sup>. We desire metrics that mimic the relative change in performance with age; therefore, the actual performance (such as the logarithm of the minimum angle of resolution, logMAR) for all age-groups has been normalized to that of the 20 to 29 age-group, as have the metric values.

Figure 7A plots the relative change in three metrics with age. Here, aberrations for each eye (Applegate et al., 2007) have been scaled to their predicted physiological pupil size for 160 cd/m<sup>2</sup> (there

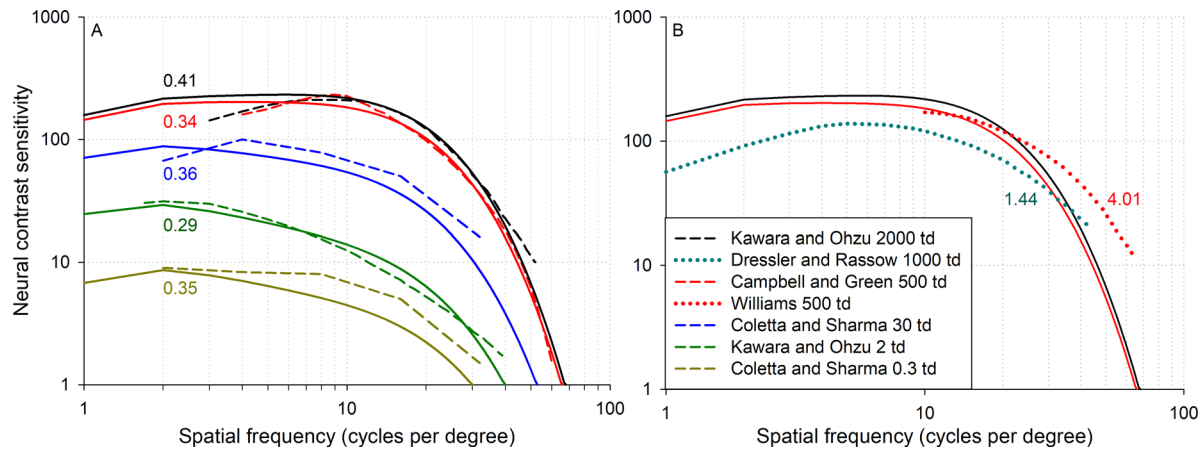


Figure 6. Comparison of the model (solid lines) with neural contrast sensitivity functions at six retinal illuminance levels extracted from (A) Figure 5 of Kawara and Ohzu (1977), Figure 5 of Campbell and Green (1965), and Figures 2d and 2g of Coletta and Sharma (1995) and from (B) Figure 5 of Williams (1985) and Figure 5 of Dressler and Rassow (1981). Model curves are for the 20 to 29 age-group; the Campbell and Green (1965) curve is for a 27-year-old. Kawara and Ohzu (1977) and Coletta and Sharma (1995) did not specify ages; the mean age of six subjects from Williams (1985) was 36 years; and Dressler and Rassow (1981) pooled data from six age-group decades. RMS log neural contrast sensitivity differences between the model curves and literature are annotated alongside the curves.

is not a substantial difference in pupil size or retinal illuminance between 160 and 200  $\text{cd}/\text{m}^2$ ; metric values are very slightly worse at 160 than 200  $\text{cd}/\text{m}^2$ , and the conventional optical Strehl ratio has been included to illustrate the isolated effect of aberrations (only the optical component; no neural component) at physiological pupil sizes.

Although none of the metric curves tracked the age-related change perfectly, the  $VSX(td,a)$  curve (weighting the optical component with a retinal illuminance- and age-specific neural function) performs better than both  $VSX(td)$  (which considers only retinal illuminance in the weighting function) and the optical Strehl ratio. The decrease in visual image quality with age may have seemed substantial in Figure 4B, but Figure 7 illustrates that it is proportionally similar to the measured deterioration of visual acuity with age. Potential explanations of the difference between  $VSX(td,a)$  and the performance data are discussed in the Limitations section.

## Interaction and roles of optical and neural factors

The modeling presented above most closely resembled physiological visual performance as a function of age when both the optical and neural components of the visual image quality metric VSX respected changes with age. Moreover, those findings suggest that the role of the neural component becomes increasingly important as age increases. However, the roles of optical and neural factors in the senescence of visual performance is a matter of some division in the literature. This may be partly due to some confusing

classification terminology. Here we summarize some areas of literature with respect to the optical and neural components of the metrics and the modeling presented.

### Wavefront aberrations

Ocular wavefront aberrations are an optical factor that the literature generally agrees increases with age at a fixed pupil size (Applegate et al., 2007; Artal, Berrio, Guirao, & Piers, 2002; Artal, Ferro, Navarro, & Miranda, 1993; Calver, Cox, & Elliott, 1999; Guirao, Gonzalez, Redondo, Geraghty, Norrby, & Artal, 1999; McLellan, Marcos, & Burns, 2001). Some studies (Applegate et al., 2007; Calver et al., 1999; Guirao et al., 1999) suggest that this increase is mitigated by decreasing physiological pupil size, whereas others report that senile miosis did not bring older eyes to the level of young eyes (McLellan et al., 2001). The literature is divided on whether the increase in aberrations with age can (Artal et al., 1993; Artal et al., 2002; McLellan et al., 2001) or cannot (Calver et al., 1999) account for the decrease in overall visual performance.

In this study, neither the magnitude of aberrations (RMS) nor their optical interaction (combined with diffraction as measured by the Strehl ratio) (Figure 5) could explain the decrease in visual acuity with age reported in the literature (Figure 7). The aberrations of the eyes increased with age at any fixed pupil size (greater for larger fixed pupils). For physiological pupil sizes at high luminance levels aberrations increased slightly with age, and at lower luminances they decreased slightly with age. Aberrations were not measured by D. B. Elliott et al. (1995) or Owsley et al. (1983), as compared in Figure 7.

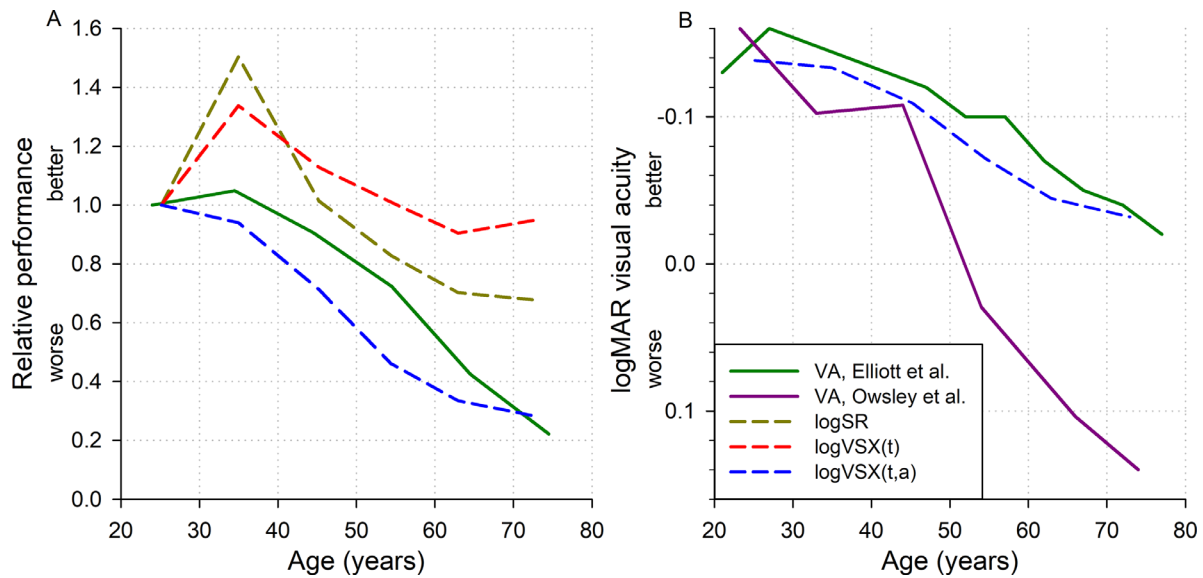


Figure 7. (A) Best-corrected (sphere, cylinder, and axis) metric values (dashed lines) as a function of age for physiological pupil sizes at  $160 \text{ cd/m}^2$  compared with logMAR visual acuity (VA) (solid line) pooled into decade age-groups from D. B. Elliott et al. (1995). All curves are normalized to the 20 to 29 age-group.  $VSX(td,a)$  (weighting the optical component with a retinal illuminance- and age-specific neural function) tracked the change in performance with age better than both  $VSX(td)$  (only accounting for retinal illuminance in the neural component) and the conventional optical Strehl ratio (no neural weighting). (B) Comparison of unpooled logMAR visual acuity from D. B. Elliott et al. (1995) with that reported by Owsley et al. (1983), which could not be normalized while maintaining proportionality as was done in panel (A) because it contains both positive and negative values. The relative change in log  $VSX(td,a)$  is drawn for comparison. For most ages, visual acuity reported by D. B. Elliott et al. (1995) is better than that predicted by  $VSX(td,a)$ , whereas that reported by Owsley et al. (1983) is worse than predicted.

## Scatter

Ocular scatter is another purely optical factor that literature generally agrees increases with age (Hennelly, Barbur, Edgar, & Woodward, 1998; van den Berg, 1995) due to inhomogeneities and increased density of ocular media (Pokorny, Smith, & Lutze, 1987; Werner, 1982). The Applegate et al. (2007) dataset excluded individuals with cortical and/or posterior subcapsular cataracts graded as  $>2$  on the LOCS-III (Chylack et al., 1993). Both reports of best-corrected visual acuity (D. B. Elliott et al., 1995; Owsley et al., 1983) with which the present modeling is compared (Figure 7) employed strict clinical screenings for ocular and systemic pathology, and eyes with substantial media opacification were similarly excluded in both cases.

Although neural processing *per se* should not be affected by lens opacities (Green, 1970), visual image quality metrics consider only optical factors measurable with wavefront aberrometry. As such, the modeling presented here is limited to healthy eyes without significant opacification. Some literature expects scatter to reduce contrast sensitivity at all spatial frequencies (D. B. Elliott, 1987), and some (D. B. Elliott, Yang, Dumbleton, & Cullen, 1993) found reduced low-contrast visual acuity, whereas others

(van den Berg, 2017) found little or no effect of scatter on visual acuity. The relation of these to visual image quality metrics remains to be studied.

## Retinal illuminance and age

Decreases and shifts in transmission (Delori & Burns, 1996; Sagawa & Takahashi, 2001; Weale, 1988) (due to media opacification and absorption) combined with senile miosis produce lower retinal illuminance with age. This is frequently considered optical, because it is caused primarily by the pupil, despite that the origin is neural, as shown when pupil size is constant (Kulikowski, 1971; Xu et al., 2017), or irrelevant, such as with Maxwellian-view interferometry (Coletta & Sharma, 1995; Kawara & Ohzu, 1977), and retinal illuminance is varied.

Using various methods to mimic the retinal processing of older eyes during contrast sensitivity testing, some studies found retinal illuminance accounted for a substantial amount (Owsley et al., 1983; Sturr, Church, & Taub, 1988; Wright & Drasdo, 1985) of age-related differences, whereas others controlled for retinal illuminance and attributed differences to neural processing (Bennett, Sekuler, & Ozin, 1999; D. Elliott, Whitaker, & MacVeigh, 1990; Higgins, Jaffe, Caruso,

& deMonasterio, 1988; Pardhan, 2004; Schefrin, Tregear, Harvey, & Werner, 1999; Sloane, Owsley, & Alvarez, 1988). The present modeling suggests that a decrease in the neural function due to retinal illuminance alone, the  $VSX(td)$  metric, is insufficient to account for the decrease in visual performance with age (Figure 7).

The present study incorporated age-related neural contrast sensitivity interferometry data (Nameda et al., 1989) into the weighting function of the  $VSX(td,a)$  metric; however, interferometry at constant retinal illuminance has also returned conflicting results. Some studies found no difference with age (Dressler & Rassow, 1981; Kayazawa, Yamamoto, & Itoi, 1981) but did not present specific data to that effect. Burton, Owsley, and Sloane (1993) found a small difference between young and old subjects, and others (D. B. Elliott, 1987; Morrison & McGrath, 1985; Nameda et al., 1989) found a more significant difference with age. Williams (1985) re-measured subject “DG” from Campbell and Green (1965) and found very little change over time from 27 to 48 years of age; however, the latter measurements were on a technologically superior interferometry system and used improved psychophysical methods that both might have compensated for age-related changes. The superior ability of the  $VSX(td,a)$  metric to track measured changes in visual acuity with age suggests substantial contributions of neural changes with age to visual processing.

Other methods that essentially bypass the ocular optics, such as contrast sensitivity through adaptive optics correction (S. Elliott et al., 2009) and displacement threshold hyperacuity (D. B. Elliott, Whitaker, & Thompson, 1989), have found differences between young and old eyes that were attributed to neural changes.

### Neuronal loss

Loss of structure does not necessarily translate to loss of function; however, an anatomical loss (or deterioration) of retinal and cortical neurons with age has been noted. Retinal ganglion cells are lost with age (Balazsi et al., 1984; Curcio & Drucker, 1993). Although change to the morphology of foveal cones has been found (Marshall, 1987), cone numbers (Curcio, Millican, Allen, & Kalina, 1993; Gao & Hollyfield, 1992) and retinal pigment epithelial cell densities (Gao & Hollyfield, 1992) are largely unchanged with age. Loss of visual cortical cells with age has been shown anatomically (Devaney & Johnson, 1980) and corroborated by electroretinogram and visual evoked potential (Porciatti et al., 1992). Although neural noise might increase with age, this has not been very extensively studied (Bennett et al., 1999; Pardhan, 2004). This structural evidence might help explain the

ability of the  $VSX(td,a)$  metric to track performance changes with age, but the relative importance and specific contributions of these constituent structural factors were not investigated.

## Limitations and applications

### Variability

Although more delineated models have been developed (Watson & Ahumada, 2005; Watson & Ahumada, 2008), visual image quality metrics consider the visual system in terms of two fundamental (optical and neural) components. Here, additional simplifications were employed. Monochromatic metrics were calculated; ocular chromatic aberration is relatively constant with age (Howarth, Zhang, Bradley, Still, & Thibos, 1988; Morrell, Whitefoot, & Charman, 1991), and the models presented here could readily be incorporated into polychromatic metric calculations (S. Ravikumar, Thibos, & Bradley, 2008); however, the spectral composition of the light reaching the retina might vary with age (Sagawa & Takahashi, 2001; Weale, 1988). We were unable to find reports of how the *oblique effect* (reduced sensitivity to obliquely oriented gratings) (Campbell, Kulikowski, & Levinson, 1966; Mitchell, Freeman, & Westheimer, 1967) varies with retinal illuminance or age. This might be expected, given that it is thought to be cortical in origin (McMahon & Macleod, 2003). Previous incorporation of the oblique effect into visual image quality metrics (Kilintari, Pallikaris, Tsiklis, & Ginis, 2010) did not significantly improve the metrics and this effect was not modeled here.

Physiological pupil sizes were predictions around which variability would be expected and would also be affected by accommodation. This variability would affect both the scaled aberrations (of the optical component) and retinal illuminance (which substantially affects the neural weighting function). Potential variability across individuals motivated the definition of the neural age multipliers in terms of decade age-groups rather than interpolating to obtain a continuous function. In the same manner that neural contrast sensitivity functions for the older age-groups were defined relative to the 20 to 29 age-group, the entire model could be shifted and defined relative to a measured function of an individual.

The objective determination of the best-corrected refractive state performed here was likely less variable than a subjectively determined best correction (Bullimore, Fusaro, & Adams, 1998; Goss & Grosvenor, 1996); however, the visual acuity data with the metric values were compared would have been affected by subjective variability (Manny, Hussein, Gwiazda,

& Marsh-Tootle, 2003; Raasch, Bailey, & Bullimore, 1998).

### Piper's law

The densities of photoreceptors and ganglion cells change substantially even within the fovea. The models of neural contrast sensitivity agreed quite well (Figure 6) with literature that used many different sized targets, despite the fact that those stimuli would have fallen over retinal areas with different sampling densities (and therefore different spatial frequency sensitivity curves). Nonetheless, the models of neural contrast sensitivity utilized by the present modeling could practically be considered unaffected by Piper's law—that is, being measured using a stimulus of sufficient extent (sufficient number of cycles) so as to be independent of stimulus area. We feel this to be a reasonable assumption given that the data of Xu et al. (2017) were made to agree with those of Campbell and Green (1965), which were measured using a 30° stimulus; therefore, at least 30 cycles were visible for all spatial frequencies tested. Literature has shown that spatial summation and, by extension, contrast sensitivity suffer when fewer than approximately eight (Robson & Graham, 1981) or ten (Howell & Hess, 1978) cycles are visible. Therefore, the modeling may not be representative of tasks that involve very small targets where spatial details are insufficiently represented. Similarly, Hoekstra, van der Goot, van den Brink, and Bilsen (1974) found that the critical number of cycles varied with target luminance, but they found that the critical number of cycles decreased (fewer visible cycles were necessary) with decreasing luminance. At all of the luminances tested by Hoekstra et al. (1974) (ranging from 2 to 600 cd/m<sup>2</sup>), the critical number of cycles appeared (from their Figure 1) to occur at fewer than 10 cycles.

### Ceiling and floor effects

The neural weighting component of visual image quality metrics such as VSX constrains the PSF to the approximate sampling and processing limits of the visual system, but a ceiling effect has been noted in how these metrics track visual performance at excellent levels of high contrast visual acuity (Applegate, Marsack, & Thibos, 2006; Villegas, Alcon, & Artal, 2008). In these cases, the metric value can be sensitive to improvements in image quality while visual acuity is unchanged at its physiological maximum. Analogously, a floor effect might exist where visual image quality degrades to a level where a change is indistinguishable to the visual system but the metric is still able to quantify the change; this remains to be investigated in future work but may be applicable to the poorest metric values in Figure 5.

Nevertheless, the  $VSX(td,a)$  metric that explicitly considered both retinal illuminance and age in the neural weighting component tracked the relative change in visual acuity with age better than did  $VSX(td)$ , which only considered age insofar as it affects retinal illuminance via senile miosis. Nameda et al. (1989) have been criticized (Burton et al., 1993) for not employing strict screening for pathology in their elderly patients; however, others (Morrison & McGrath, 1985) found comparable results. An ideal dataset would have contained aberrations, best-corrected performance, and a measure of neural processing such as neural contrast sensitivity, all as a function of retinal illuminance and age, all on the same individuals; unfortunately, these were not available. When combining and comparing data from multiple sources, making manual modifications (say, to the weighting functions) could easily have been erroneously influenced by an idiosyncrasy of another dataset; therefore, this was not done. In contrast, we sought to base the models in the literature.

Ultimately, the models of neural contrast sensitivity presented here can easily be incorporated into existing visual image quality metric calculations (Appendix B) as well as into other modeling of foveal vision and visual processing. Although the Campbell and Green (1965) function has been adequate at high photopic levels, the presented models allow the neural weighting component of visual image quality metrics to better respect how retinal illuminance and age impact the neural contrast sensitivity function and, in doing so, allow the metrics to better track the change in visual performance with age.

## Conclusions

Physiological visual image quality was modeled as a function of target luminance and age, where the optical component (aberrations) of the metric was scaled to physiological pupil sizes, and two models of neural contrast sensitivity as a function of (1) retinal illuminance and (2) retinal illuminance and age were constructed from the literature and incorporated into the neural component of the metric calculation. The optical and neural components interacted in three ways that depended on luminance, and the role of the neural component became increasingly relevant as age increased. Weighting the optical component with a neural function that considered both retinal illuminance and age allowed objectively best-corrected metric values at physiological pupil sizes to track measured best-corrected visual acuity as a function of age better than a model that accounted only for retinal illuminance and better than a purely optical model (no neural weighting).

*Keywords:* visual image quality, neural contrast sensitivity, luminance, aging, Trolands

## Acknowledgments

The authors thank David Williams, Arthur Bradley, and Daniel Coates for helpful discussions, as well as the managing editor and two anonymous reviewers for adding great value to the manuscript.

Supported by grants from the National Institutes of Health/National Eye Institute (R01EY008520 to RAA; R01EY019105 to JDM and RAA; and core grant P30EY07551 to UH); U.S. Navy Subcontract N00259-10-P-1354; and the Borish Endowment (RAA). Portions of these findings were presented at the International Congress on Wavefront and Presbyopic Corrections, Sante Fe, NM, March 2019, and at the Association for Research in Vision and Ophthalmology, Vancouver, Canada, April 2019.

Commercial relationships: none.

Corresponding author: Gareth D. Hastings.

Email: gdhastings1@gmail.com.

Address: School of Optometry, University of California, Berkeley, CA, USA.

## References

- American National Standards Institute. (2004). *American National Standard for Ophthalmics: Methods for reporting optical aberrations of eyes, ANSI Z80.28–2004*. Merrifield, VA: Optical Laboratory Association.
- Applegate, R., Donnelly, W., III, Marsack, J., Koenig, D., & Pesudovs, K. (2007). Three-dimensional relationship between high-order root-mean-square wavefront error, pupil diameter, and aging. *Journal of the Optical Society of America A. Optics, Image Science, and Vision*, 24(3), 578–587.
- Applegate, R., Marsack, J., & Thibos, L. (2006). Metrics of retinal image quality predict visual performance in eyes with 20/17 or better visual acuity. *Optometry and Vision Science*, 83(9), 635–640.
- Artal, P., Berrio, E., Guirao, A., & Piers, P. (2002). Contribution of the cornea and internal surfaces to the change of ocular aberrations with age. *Journal of the Optical Society of America A. Optics, Image Science, and Vision*, 19(1), 137–143, <https://doi.org/10.1364/JOSAA.19.000137>.
- Artal, P., Ferro, M., Navarro, R., & Miranda, I. (1993). Effects of aging in retinal image quality. *Journal of the Optical Society of America A. Optics, Image Science, and Vision*, 10(7), 1656–1662.
- Balazsi, A., Rootman, J., Drance, S., Schulzer, M., & Douglas, G. (1984). The effect of age on the nerve fiber population of the human optic nerve. *American Journal of Ophthalmology*, 97(6), 760–766.
- Banks, M., Geisler, W., & Bennett, P. (1987). The physical limits of grating visibility. *Vision Research*, 27(11), 1915–1924, [https://doi.org/10.1016/0042-6989\(87\)90057-5](https://doi.org/10.1016/0042-6989(87)90057-5).
- M. Bass (Ed.). (1995). *Handbook of optics* (2nd ed.). New York: McGraw-Hill.
- Bennett, P., Sekuler, A., & Ozin, L. (1999). Effects of aging on calculation efficiency and equivalent noise. *Journal of the Optical Society of America A. Optics, Image Science, and Vision*, 16(3), 654, <https://doi.org/10.1364/JOSAA.16.000654>.
- Bonaque-González, S., Ríos, S., Amigó, A., & López-Gil, N. (2015). Influence on visual quality of intraoperative orientation of asymmetric intraocular lenses. *Journal of Refractive Surgery*, 31(10), 651–657, <https://doi.org/10.3928/1081597X-20150922-01>.
- Brunette, I., Bueno, J. M., Parent, M., Hamam, H., & Simonet, P. (2003). Monochromatic aberrations as a function of age, from childhood to advanced age. *Investigative Ophthalmology & Visual Science*, 44(12), 5438–5446, <https://doi.org/10.1167/iovs.02-1042>.
- Bühren, J., Yoon, G., MacRae, S., & Huxlin, K. (2010). Contribution of optical zone decentration and pupil dilation on the change of optical quality after myopic photorefractive keratectomy in a cat model. *Journal of Refractive Surgery*, 26(3), 183–190, <https://doi.org/10.3928/1081597X-20100224-04>.
- Bullimore, M., Fusaro, R., & Adams, C. (1998). The repeatability of automated and clinician refraction. *Optometry and Vision Science*, 75(8), 617–622.
- Burton, K., Owsley, C., & Sloane, M. (1993). Aging and neural spatial contrast sensitivity: photopic vision. *Vision Research*, 33(7), 939–946.
- Calver, R., Cox, M., & Elliott, D. (1999). Effect of aging on the monochromatic aberrations of the human eye. *Journal of the Optical Society of America A. Optics, Image Science, and Vision*, 16(9), 2069–2078.
- Campbell, F., & Green, D. (1965). Optical and retinal factors affecting visual resolution. *Journal of Physiology*, 181(3), 576–593.
- Campbell, F., Kulikowski, J., & Levinson, J. (1966). The effect of orientation on the visual resolution of gratings. *Journal of Physiology*, 187(2), 427–436.
- Candy, T., Wang, J., & Ravikumar, S. (2009). Retinal image quality and postnatal visual

- experience during infancy. *Optometry and Vision Science*, 86(6), E556–E571, <https://doi.org/10.1097/OPX.0b013e3181a76e6f>.
- Chen, L., Singer, B., Guirao, A., Porter, J., & Williams, D. (2005). Image metrics for predicting subjective image quality. *Optometry and Vision Science*, 82(5), 358–369.
- Cheng, X., Bradley, A., Ravikumar, S., & Thibos, L. (2010). The visual impact of Zernike and Seidel forms of monochromatic aberrations. *Optometry and Vision Science*, 87(5), 300–312.
- Cheng, X., Bradley, A., & Thibos, L. (2004). Predicting subjective judgment of best focus with objective image quality metrics. *Journal of Vision*, 4(4), 310–321, <https://doi.org/10.1167/4.4.7>.
- Chylack, L., Wolfe, J., Singer, D., Leske, M., Bullimore, M., & Bailey, I., ..., Wu, S. (1993). The Lens Opacities Classification System III. *Archives of Ophthalmology*, 111(6), 831, <https://doi.org/10.1001/archophth.1993.01090060119035>.
- Coletta, N., & Sharma, V. (1995). Effects of luminance and spatial noise on interferometric contrast sensitivity. *Journal of the Optical Society of America A. Optics, Image Science, and Vision*, 12(10), 2244–2251.
- Collins, M., Buehren, T., & Iskander, D. (2006). Retinal image quality, reading and myopia. *Vision Research*, 46(1–2), 196–215, <https://doi.org/10.1016/j.visres.2005.03.012>.
- Curcio, C., & Drucker, D. (1993). Retinal ganglion cells in Alzheimer's disease and aging. *Annals of Neurology*, 33, 248–257.
- Curcio, C., Millican, C., Allen, K., & Kalina, R. (1993). Aging of the human photoreceptor mosaic: Evidence for selective vulnerability of rods in central retina. *Investigative Ophthalmology & Visual Science*, 34(12), 3278–3296.
- Delori, F., & Burns, S. (1996). Fundus reflectance and the measurement of crystalline lens density. *Journal of the Optical Society of America A. Optics, Image Science, and Vision*, 13(2), 215, <https://doi.org/10.1364/JOSAA.13.000215>.
- D'Errico, J. (2016). polyfitn. Available at: <https://www.mathworks.com/matlabcentral/fileexchange/34765-polyfitn>. Accessed November 06, 2017.
- Devaney, K., & Johnson, H. (1980). Neuron loss in the aging visual cortex of man. *Journal of Gerontology*, 35(6), 836–841.
- Dressler, M., & Rassow, B. (1981). Neural contrast sensitivity measurements with a laser interference system for clinical and screening application. *Investigative Ophthalmology & Visual Science*, 21(5), 737–744.
- Elliott, D., Whitaker, D., & MacVeigh, D. (1990). Neural contribution to spatiotemporal contrast sensitivity decline in healthy ageing eyes. *Vision Research*, 30(4), 541–547, [https://doi.org/10.1016/0042-6989\(90\)90066-T](https://doi.org/10.1016/0042-6989(90)90066-T).
- Elliott, D. B. (1987). Contrast sensitivity decline with ageing: a neural or optical phenomenon? *Ophthalmic & Physiological Optics*, 7(4), 415–419.
- Elliott, D. B., Whitaker, D., & Thompson, P. (1989). Use of displacement threshold hyperacuity to isolate the neural component of senile vision loss. *Applied Optics*, 28(10), 1914–1918, <https://doi.org/10.1364/AO.28.001914>.
- Elliott, D. B., Yang, K., Dumbleton, K., & Cullen, A. (1993). Ultraviolet-induced lenticular fluorescence: Intraocular straylight affecting visual function. *Vision Research*, 33(13), 1827–1833, [https://doi.org/10.1016/0042-6989\(93\)90173-T](https://doi.org/10.1016/0042-6989(93)90173-T).
- Elliott, D. B., Yang, K., & Whitaker, D. (1995). Visual acuity changes throughout adulthood in normal, healthy eyes: seeing beyond 6/6. *Optometry and Vision Science*, 72(3), 186–191.
- Elliott, S., Choi, S., Doble, N., Hardy, J., Evans, J., & Werner, J. (2009). Role of high-order aberrations in senescent changes in spatial vision. *Journal of Vision*, 9(2), 1–16, <https://doi.org/10.1167/9.2.24>.
- Gao, H., & Hollyfield, J. (1992). Differential loss of neurons and retinal pigment epithelial cells. *Investigative Ophthalmology & Visual Science*, 33(1), 1–17.
- Goodman, J. (1996). *Introduction to Fourier optics* (2nd ed.). New York: McGraw-Hill.
- Goss, D., & Grosvenor, T. (1996). Reliability of refraction—a literature review. *Journal of the American Optometric Association*, 67(10), 619–630.
- Green, D. (1970). Testing the vision of cataract patients by means of laser-generated interference fringes. *Science*, 168(3936), 1240–1242.
- Guirao, A., Gonzalez, C., Redondo, M., Geraghty, E., Norrby, S., & Artal, P. (1999). Average optical performance of the human eye as a function of age in a normal population. *Investigative Ophthalmology & Visual Science*, 40(1), 203–213.
- Hastings, G., Applegate, R., Nguyen, L., Kauffman, M., Hemmati, R., & Marsack, J. (2019). Comparison of wavefront-guided and best conventional scleral lenses after habituation in eyes with corneal ectasia. *Optometry and Vision Science*, 96(4), 238–247, <https://doi.org/10.1097/OPX.0000000000001365>.
- Hastings, G., Marsack, J., Nguyen, L., Cheng, H., & Applegate, R. (2017). Is an objective refraction optimised using the visual Strehl

- ratio better than a subjective refraction? *Ophthalmic & Physiological Optics*, 37(3), 317–325, <https://doi.org/10.1111/opo.12363>.
- Hastings, G., Marsack, J., Thibos, L., & Applegate, R. (2018). Normative best-corrected values of the visual image quality metric VSX as a function of age and pupil size. *Journal of the Optical Society of America A. Optics, Image Science, and Vision*, 35(5), 732–739, <https://doi.org/10.1364/JOSAA.35.000732>.
- Hastings, G., Zanayed, J., Nguyen, L., Applegate, R., & Marsack, J. (2020). Do polymer coatings change the aberrations of conventional and wavefront-guided scleral lenses? *Optometry and Vision Science*, 97(1), 28–35, <https://doi.org/10.1097/OPX.0000000000001462>.
- Hennelly, M., Barbur, J., Edgar, D., & Woodward, E. (1998). The effect of age on the light scattering characteristics of the eye. *Ophthalmic & Physiological Optics*, 18(2), 197–203.
- Higgins, K., Jaffe, M., Caruso, R., & deMonasterio, F. (1988). Spatial contrast sensitivity: Effects of age, test–retest, and psychophysical method. *Journal of the Optical Society of America A. Optics, Image Science, and Vision*, 5(12), 2173–2180, <https://doi.org/10.1364/JOSAA.5.002173>.
- Hoekstra, J., van der Goot, D., van den Brink, G., & Bilsen, F. (1974). The influence of the number of cycles upon the visual contrast threshold for spatial sine wave patterns. *Vision Research*, 14(6), 365–368, [https://doi.org/10.1016/0042-6989\(74\)90234-x](https://doi.org/10.1016/0042-6989(74)90234-x).
- Howarth, P., Zhang, X., Bradley, A., Still, D., & Thibos, L. (1988). Does the chromatic aberration of the eye vary with age? *Journal of the Optical Society of America A. Optics, Image Science, and Vision*, 5(12), 2087–2092, <https://doi.org/10.1364/JOSAA.5.002087>.
- Howell, E., & Hess, R. (1978). The functional area for summation to threshold for sinusoidal gratings. *Vision Research*, 18(4), 369–374, [https://doi.org/10.1016/0042-6989\(78\)90045-7](https://doi.org/10.1016/0042-6989(78)90045-7).
- Kawara, T., & Ohzu, H. (1977). Modulation transfer function of human visual system. *Oyobutsuri (Japan)*, 46, 128–138.
- Kayazawa, F., Yamamoto, T., & Itoi, M. (1981). Clinical measurement of contrast sensitivity function using laser generated sinusoidal grating. *Japanese Journal of Ophthalmology*, 25, 229–236.
- Kilintari, M., Pallikaris, A., Tsiklis, N., & Ginis, H. (2010). Evaluation of image quality metrics for the prediction of subjective best focus. *Optometry and Vision Science*, 87(3), 183–189.
- Kulikowski, J. (1971). Some stimulus parameters affecting spatial and temporal resolution of human vision. *Vision Research*, 11(1), 83–93, [https://doi.org/10.1016/0042-6989\(71\)90206-9](https://doi.org/10.1016/0042-6989(71)90206-9).
- Liu, T., & Thibos, L. (2019). Customized models of ocular aberrations across the visual field during accommodation. *Journal of Vision*, 19(9), 13, <https://doi.org/10.1167/19.9.13>.
- Liu, T., Wang, Z.-Q., Wang, Y., Mu, G.-G., & Zhao, K.-X. (2010). Measurements of retinal aerial image modulation (AIM) for white light based on wave-front aberration of human eye. *Optik*, 121(1), 101–106, <https://doi.org/10.1016/j.ijleo.2008.05.021>.
- López-Gil, N., Martin, J., Liu, T., Bradley, A., Díaz-Muñoz, D., & Thibos, L. (2013). Retinal image quality during accommodation. *Ophthalmic & Physiological Optics*, 33(4), 497–507, <https://doi.org/10.1111/opo.12075>.
- Manny, R., Hussein, M., Gwiazda, J., & Marsh-Tootle, W. (2003). Repeatability of ETDRS visual acuity in children. *Investigative Ophthalmology & Visual Science*, 44(8), 3294–3300, <https://doi.org/10.1167/iovs.02-1199>.
- Marsack, J., Thibos, L., & Applegate, R. (2004). Metrics of optical quality derived from wave aberrations predict visual performance. *Journal of Vision*, 4(4), 322–328, <https://doi.org/10.1167/4.4.8>.
- Marshall, J. (1987). The ageing retina: Physiology or pathology. *Eye*, 1(2), 282–295, <https://doi.org/10.1038/eye.1987.47>.
- Martin, J., Vasudevan, B., Himebaugh, N., Bradley, A., & Thibos, L. (2011). Unbiased estimation of refractive state of aberrated eyes. *Vision Research*, 51(17), 1932–1940, <https://doi.org/10.1016/j.visres.2011.07.006>.
- McLellan, J. S., Marcos, S., & Burns, S. A. (2001). Age-related changes in monochromatic wave aberrations of the human eye. *Investigative Ophthalmology & Visual Science*, 42(6), 1390–1395.
- McMahon, M. J., & Macleod, D. I. (2003). The origin of the oblique effect examined with pattern adaptation and masking. *Journal of Vision*, 3(3), 230–239.
- Michael, R., Guevara, O., de la Paz, M., Alvarez de Toledo, J., & Barraquer, R. (2011). Neural contrast sensitivity calculated from measured total contrast sensitivity and modulation transfer function. *Acta Ophthalmologica*, 89(3), 278–283, <https://doi.org/10.1111/j.1755-3768.2009.01665.x>.
- Mitchell, D., Freeman, R., & Westheimer, G. (1967). Effect of orientation on the modulation sensitivity for interference fringes on the retina. *Journal of the Optical Society of America A. Optics, Image Science, and Vision*, 57(2), 246–249.

- Morrell, A., Whitefoot, H., & Charman, W. (1991). Ocular chromatic aberration and age. *Ophthalmic & Physiological Optics*, 11(4), 385–390.
- Morrison, J., & McGrath, C. (1985). Assessment of the optical contributions to the age-related deterioration in vision. *Quarterly Journal of Experimental Physiology*, 70(2), 249–269.
- Movshon, J., & Kiorpes, L. (1988). Analysis of the development of spatial contrast sensitivity in monkey and human infants. *Journal of the Optical Society of America A. Optics, Image Science, and Vision*, 5(12), 2166–2172, <https://doi.org/10.1364/JOSAA.5.002166>.
- Nameda, N., Kawara, T., & Ohzu, H. (1989). Human visual spatio-temporal frequency performance as a function of age. *Optometry and Vision Science*, 66(11), 760–765.
- Owsley, C., Sekuler, R., & Siemsen, D. (1983). Contrast sensitivity throughout adulthood. *Vision Research*, 23(7), 689–699.
- Pardhan, S. (2004). Contrast sensitivity loss with aging: sampling efficiency and equivalent noise at different spatial frequencies. *Journal of the Optical Society of America A. Optics, Image Science, and Vision*, 21(2), 169–175, <https://doi.org/10.1364/JOSAA.21.000169>.
- Pokorny, J., Smith, V., & Lutze, M. (1987). Aging of the human lens. *Applied Optics*, 26(8), 1437–1440, <https://doi.org/10.1364/AO.26.001437>.
- Porciatti, V., Burr, D., Morrone, M., & Fiorentini, A. (1992). The effects of ageing on the pattern electroretinogram and visual evoked potential in humans. *Vision Research*, 32(7), 1199–1209, [https://doi.org/10.1016/0042-6989\(92\)90214-4](https://doi.org/10.1016/0042-6989(92)90214-4).
- Raasch, T., Bailey, I., & Bullimore, M. (1998). Repeatability of visual acuity measurement. *Optometry and Vision Science*, 75(5), 342–348.
- Ravikumar, A., Applegate, R., Shi, Y., & Bedell, H. (2011). Six just-noticeable differences in retinal image quality in 1 line of visual acuity: Toward quantification of happy versus unhappy patients with 20/20 acuity. *Journal of Cataract & Refractive Surgery*, 37(8), 1523–1529, <https://doi.org/10.1016/j.jcrs.2011.02.034>.
- Ravikumar, A., Benoit, J., Marsack, J., & Anderson, H. (2019). Image quality metric derived refractions predicted to improve visual acuity beyond habitual refraction for patients with Down syndrome. *Translational Vision Science & Technology*, 8(3), 20, <https://doi.org/10.1167/tvst.8.3.20>.
- Ravikumar, A., Sarver, E., & Applegate, R. (2012). Change in visual acuity is highly correlated with change in six image quality metrics independent of wavefront error and/or pupil diameter. *Journal of Vision*, 12(10), 11, <https://doi.org/10.1167/12.10.11>.
- Ravikumar, S., Thibos, L., & Bradley, A. (2008). Calculation of retinal image quality for polychromatic light. *Journal of the Optical Society of America A. Optics, Image Science, and Vision*, 25(10), 2395–2407.
- Robson, J., & Graham, N. (1981). Probability summation and regional variation in contrast sensitivity across the visual field. *Vision Research*, 21(3), 409–418, [https://doi.org/10.1016/0042-6989\(81\)90169-3](https://doi.org/10.1016/0042-6989(81)90169-3).
- Roufs, J. A. J. (1978). *Light as a true visual quantity: Principles of measurement*. Paris: Commission Internationale l’Eclairage.
- Rovamo, J., Mustonen, J., & Näsänen, R. (1994). Modelling contrast sensitivity as a function of retinal illuminance and grating area. *Vision Research*, 34(10), 1301–1314.
- Sabesan, R., Barbot, A., & Yoon, G. (2017). Enhanced neural function in highly aberrated eyes following perceptual learning with adaptive optics. *Vision Research*, 132, 78–84, <https://doi.org/10.1016/j.visres.2016.07.011>.
- Sagawa, K., & Takahashi, Y. (2001). Spectral luminous efficiency as a function of age. *Journal of the Optical Society of America A. Optics, Image Science, and Vision*, 18(11), 2659–2667, <https://doi.org/10.1364/JOSAA.18.002659>.
- Schefrin, B. E., Tregear, S. J., Harvey, L. O., & Werner, J. S. (1999). Senescent changes in scotopic contrast sensitivity. *Vision Research*, 39(22), 3728–3736, [https://doi.org/10.1016/S0042-6989\(99\)00072-3](https://doi.org/10.1016/S0042-6989(99)00072-3).
- Schoneveld, P., Pesudovs, K., & Coster, D. (2009). Predicting visual performance from optical quality metrics in keratoconus. *Clinical and Experimental Optometry*, 92(3), 289–296, <https://doi.org/10.1111/j.1444-0938.2009.00372.x>.
- Schwiegerling, J. (2002). Scaling Zernike expansion coefficients to different pupil sizes. *Journal of the Optical Society of America A. Optics, Image Science, and Vision*, 19(10), 1937–1945.
- Shi, Y., Applegate, R. A., Wei, X., Ravikumar, A., & Bedell, H. E. (2013a). Registration tolerance of a custom correction to maintain visual acuity. *Optometry and Vision Science*, 90(12), 1370–1384.
- Shi, Y., Queener, H. M., Marsack, J. D., Ravikumar, A., Bedell, H. E., & Applegate, R. A. (2013b). Optimizing wavefront-guided corrections for highly aberrated eyes in the presence of registration uncertainty. *Journal of Vision*, 13(7), 8, <https://doi.org/10.1167/13.7.8>.
- Sloane, M., Owsley, C., & Alvarez, S. (1988a). Aging, senile miosis and spatial contrast sensitivity at low luminance. *Vision Research*, 28(11), 1235–1246, [https://doi.org/10.1016/0042-6989\(88\)90039-9](https://doi.org/10.1016/0042-6989(88)90039-9).

- Sloane, M., Owsley, C., & Jackson, C. (1988b). Aging and luminance-adaptation effects on spatial contrast sensitivity. *Journal of the Optical Society of America A. Optics, Image Science, and Vision*, 5(12), 2181–2190, <https://doi.org/10.1364/JOSAA.5.002181>.
- Sreenivasan, V., Aslakson, E., Kornaus, A., & Thibos, L. N. (2013). Retinal image quality during accommodation in adult myopic eyes. *Optometry and Vision Science*, 90(11), 1292–1303.
- Still, D. (1989). *Optical limits to contrast sensitivity in human peripheral vision* (UMI #9020696). Bloomington, IN: Indiana University.
- Sturr, J., Church, K., & Taub, H. (1988). Temporal summation functions for detection of sine-wave gratings in young and older adults. *Vision Research*, 28(11), 1247–1253, [https://doi.org/10.1016/0042-6989\(88\)90040-5](https://doi.org/10.1016/0042-6989(88)90040-5).
- Thibos, L., Hong, X., Bradley, A., & Applegate, R. (2004). Accuracy and precision of objective refraction from wavefront aberrations. *Journal of Vision*, 4(4), 329–351, <https://doi.org/10.1167/4.4.9>.
- van den Berg, T. (1995). Analysis of intraocular straylight, especially in relation to age. *Optometry and Vision Science*, 72(2), 52–59.
- van den Berg, T. (2017). The (lack of) relation between straylight and visual acuity. Two domains of the point-spread-function. *Ophthalmic & Physiological Optics*, 37(3), 333–341, <https://doi.org/10.1111/opo.12368>.
- Van Nes, F., & Bouman, M. (1967). Spatial modulation transfer in the human eye. *Journal of the Optical Society of America*, 57(3), 401–406, <https://doi.org/10.1364/JOSA.57.000401>.
- Villegas, E., Alcon, E., & Artal, P. (2008). Optical quality of the eye in subjects with normal and excellent visual acuity. *Investigative Ophthalmology & Visual Science*, 49(10), 4688–4696, <https://doi.org/10.1167/iovs.08-2316>.
- Watson, A., & Ahumada, A. (2005). A standard model for foveal detection of spatial contrast. *Journal of Vision*, 5(9), 714–740.
- Watson, A., & Ahumada, A. (2008). Predicting visual acuity from wavefront aberrations. *Journal of Vision*, 8(4), 17.1–19, <https://doi.org/10.1167/8.4.17>.
- Watson, A., & Yellott, J. (2012). A unified formula for light-adapted pupil size. *Journal of Vision*, 12(10), 12, <https://doi.org/10.1167/12.10.12>.
- Weale, R. (1988). Age and the transmittance of the human crystalline lens. *The Journal of Physiology*, 395(1), 577–587, <https://doi.org/10.1113/jphysiol.1988.sp016935>.
- Wensveen, J., Smith, E., Hung, L., & Harwerth, R. (2011). Brief daily periods of unrestricted vision preserve stereopsis in strabismus. *Investigative Ophthalmology & Visual Science*, 52(7), 4872–4879, <https://doi.org/10.1167/iovs.10-6891>.
- Werner, J. (1982). Development of scotopic sensitivity and the absorption spectrum of the human ocular media. *J Opt Soc Am*, 72(2), 247–258, <https://doi.org/10.1364/JOSA.72.000247>.
- Williams, D. R. (1985). Visibility of interference fringes near the resolution limit. *Journal of the Optical Society of America A. Optics, Image Science, and Vision*, 2(7), 1087–1093.
- Wilson, H. (1978). Quantitative prediction of line spread function measurements: Implications for channel bandwidths. *Vision Research*, 18(4), 493–496, [https://doi.org/10.1016/0042-6989\(78\)90062-7](https://doi.org/10.1016/0042-6989(78)90062-7).
- Wright, C., & Drasdo, N. (1985). The influence of age on the spatial and temporal contrast sensitivity function. *Documenta Ophthalmologica*, 59(4), 385–395, <https://doi.org/10.1007/BF00159172>.
- Wyszecki, G., & Stiles, W. S. (2000). *Color science: Concepts and methods, quantitative data, and formulae* (2nd ed.). New York: John Wiley & Sons.
- Xu, R., Wang, H., Thibos, L., & Bradley, A. (2017). Interaction of aberrations, diffraction, and quantal fluctuations determine the impact of pupil size on visual quality. *Journal of the Optical Society of America A. Optics, Image Science, and Vision*, 34(4), 481–492, <https://doi.org/10.1364/JOSAA.34.000481>.
- Yi, F., Iskander, D., & Collins, M. (2010). Estimation of the depth of focus from wavefront measurements. *Journal of Vision*, 10(4), 1–9, <https://doi.org/10.1167/10.4.3>.
- Yoss, R., Moyer, N., & Hollenhorst, R. (1970). Pupil size and spontaneous pupillary waves associated with alertness, drowsiness, and sleep. *Neurology*, 20(6), 545–554, <https://doi.org/10.1212/wnl.20.6.545>.

## Appendix A: Calculated and actual dilated pupil diameters

All mean  $\pm$  standard deviation pupil sizes are diameters expressed in millimeters. At target luminances between 4 and 1 log cd/m<sup>2</sup>, the dilated pupil size of each eye was greater than the calculated physiological pupil size (Watson & Yellott, 2012). At lower target luminances, a small proportion of eyes did not dilate to the calculated pupil size, and the actual dilated pupil size was used instead to avoid scaling aberrations to a larger pupil size than was measured.

## Appendix B: MATLAB code to generate neural contrast sensitivity as a function of retinal illuminance and age

Please see Supplementary MATLAB file *nCSF\_model.m*.

Luminance	Pupil	Age-group					
		20–29 y(n = 20)	30–39 y(n = 18)	40–49 y(n = 32)	50–59 y(n = 32)	60–69 y(n = 21)	70–79 y(n = 23)
4 log cd/m <sup>2</sup>	Calculated pupil, mm	2.70 ± 0.01	2.66 ± 0.01	2.61 ± 0.01	2.57 ± 0.01	2.54 ± 0.01	2.49 ± 0.01
3 log cd/m <sup>2</sup>	Calculated pupil, mm	3.53 ± 0.03	3.41 ± 0.03	3.41 ± 0.03	3.29 ± 0.03	3.18 ± 0.03	3.07 ± 0.02
2 log cd/m <sup>2</sup>	Calculated pupil, mm	4.80 ± 0.05	4.56 ± 0.06	4.32 ± 0.07	4.10 ± 0.07	3.90 ± 0.05	3.66 ± 0.06
1 log cd/m <sup>2</sup>	Calculated pupil, mm	6.13 ± 0.08	5.78 ± 0.09	5.41 ± 0.10	5.08 ± 0.10	4.77 ± 0.07	4.41 ± 0.09
0 log cd/m <sup>2</sup>	Calculated pupil, mm	7.07 ± 0.10	6.63 ± 0.11	6.17 ± 0.13	5.76 ± 0.13	5.38 ± 0.09	4.93 ± 0.11
	Actual pupil, mm	7.03 ± 0.15	6.63 ± 0.11	6.17 ± 0.13	5.76 ± 0.13	5.38 ± 0.09	4.93 ± 0.11
	Mean difference, mm	0.04	0.00	0.00	0.00	0.00	0.00
	No. eyes where actual pupil size < calculated	2	2	0	0	0	0
–1 log cd/m <sup>2</sup>	Calculated pupil, mm	7.56 ± 0.11	7.08 ± 0.12	6.57 ± 0.14	6.12 ± 0.14	5.70 ± 0.10	5.20 ± 0.12
	Actual pupil, mm	7.47 ± 0.29	7.00 ± 0.17	6.55 ± 0.16	6.11 ± 0.15	5.70 ± 0.10	5.20 ± 0.12
	Mean difference, mm	0.10	0.08	0.02	0.00	0.00	0.00
	No. eyes where actual pupil size < calculated	3	4	2	1	0	0
–2 log cd/m <sup>2</sup>	Calculated pupil, mm	7.78 ± 0.12	7.28 ± 0.12	6.75 ± 0.14	6.28 ± 0.15	5.84 ± 0.10	5.33 ± 0.12
	Actual pupil, mm	7.64 ± 0.35	7.15 ± 0.24	6.71 ± 0.19	6.26 ± 0.17	5.84 ± 0.10	5.33 ± 0.12
	Mean difference, mm	0.14	0.13	0.04	0.01	0.00	0.00
	No. eyes where actual pupil size < calculated	4	5	3	3	1	0
–3 log cd/m <sup>2</sup>	Calculated pupil, mm	7.87 ± 0.12	7.36 ± 0.13	6.82 ± 0.15	6.34 ± 0.15	5.90 ± 0.10	5.38 ± 0.13
	Actual pupil, mm	7.72 ± 0.38	7.20 ± 0.27	6.78 ± 0.21	6.32 ± 0.18	5.89 ± 0.10	5.38 ± 0.12
	Mean difference, mm	0.16	0.15	0.04	0.02	0.01	0.00
	No. eyes where actual pupil size < calculated	4	6	3	3	1	0